RADON-222 TRANSPORT INTO OPEN AIR FROM A PHOSPHOGYPSUM STACK: NUMERICAL SIMULATION FOR DIFFERENT ASPECT RATIOS

José Antonio Rabi
FZEA / USP – Faculty of Zootechny and Food Engineering, University of Sao Paulo
Av. Duque de Caxias Norte, 225, Pirassununga, SP, 13635-900, Brazil
e-mail: jrabi@fzea.usp.br

Abstract. *Stack disposal of phosphogypsum copes with environmental issues concerning radon-222 transport into local atmosphere. An existing finite-volume computational simulator for heat and mass transfer in media fully or partially filled with porous matrix has been continuously adapted to predict radon-222 exhalation rates from phosphogypsum-bearing materials. This paper numerically investigates the effect of different aspect ratios on the steady-state two-dimensional natural-convective transfer of such gaseous radionuclide from a phosphogypsum stack into surrounding air. The supposedly laminar buoyancy-driven fluid flow is modeled following Darcy-Brinkman-Boussinesq approach while the stack is approximated as a dry rectangular porous matrix with uniform porosity and isotropic permeability. Differential governing equations are cast in dimensionless form so as to encompass simultaneous effects from entailed physical parameters. Besides the aspect ratio, Darcy number is allowed to vary for exploratory purposes whereas the remaining controlling groups are fixed at representative values. Heat and species (radon-222 activity) transfer rates are expressed by means of suitably defined Nusselt and Sherwood numbers respectively. Numerical results are compared to an attainable analytical solution corresponding to a stratified limiting scenario.*

Keywords*: mass transfer, porous media, numerical simulation, phosphogypsum, radon-222*

1. Introduction

Phosphogypsum ($CaSO_4 \cdot 2H_2O$) is a by-product from phosphate fertilizer industries with little (if any) economic value. As a result, huge amounts of such waste have been simply disposed off in stacks nearby industrial units, raising environmental concerns related to ^{222}Rn exhalation. Belonging to the ^{238}U chain, ^{222}Rn results from the α-decay of ^{226}Ra, which is a radionuclide commonly found in phosphogypsum as an impurity. In view of that, ^{226}Ra trapped within phosphogypsum decays to ^{222}Rn, which is able to percolate through stack layers, reach up the open atmosphere and finally be inhaled by nearby humans. While the progeny of this radioactive noble gas is likely to decay to ^{210}Pb before being removed by clearance mechanisms, higher lung cancer risk has been assigned to the radiation released by those short-lived decay products (Nero, 1988). Along with its short-lived decay products, ^{222}Rn responds to most of human exposure to radiation from natural sources (UNSCEAR, 2000).

Understanding ^{222}Rn generation and transport in porous media can be useful to analyze environmental issues related to phosphogypsum because radiological protection design is based on ^{222}Rn exhalation rates. Researches have been conducted so as to measure ^{222}Rn concentration in air, correlating it to involved physical parameters such as emanation rate, moisture content, temperature, mass diffusivity, material porosity and permeability. Models for ^{222}Rn transport in porous media have considered both diffusion and convection though early models have basically accounted for air flow driven by pre-defined pressures differences and Darcy's law (Loureiro, 1987; Yu *et al.*, 1993). This approach has yet been followed (Riley *et al.*, 1999; Andersen, 2000) as it yields a Poisson (transient) or a Laplace (steady-state) transport equation to be solved for pressure instead of separate momentum equations, which simplifies numerical implementation of related transport equations into computational code.

An existing finite-volume simulator has been continuously improved to simulate comprehensive ^{222}Rn generation and transport in porous media (Rabi and Mohamad, 2005). Accordingly, this paper considers two-dimensional steady-state diffusive-convective ^{222}Rn transport from a phosphogypsum stack, where buoyancy-driven air flow follows Darcy-Brinkman-Boussinesq approach. As an attempt to deal with concurrent effects of entailed physical factors, governing equations are written in dimensionless form and numerically solved with the help of the aforesaid simulator so that ^{222}Rn exhalation rates from the stack into local air can be predicted. Effects of different aspect ratios are investigated for two distinct Darcy numbers (i.e., stack permeabilities).

2. Test case definition and dimensionless mathematical modeling

A representative elementary volume (REV) in a phosphogypsum stack may comprise grains and interstices filled up with air and water. Although the cross-section of a stack usually assumes a trapezoidal shape, as sketched in Fig. 1(a), this paper approximates it by a rectangle of aspect ratio A (= half-width / height), as shown in Fig. 1(b) along with related dimensionless Cartesian coordinates. The stack is regarded sufficiently large in the direction normal to the plane of Fig. 1(b), composed of dry phosphogypsum whose porosity and isotropic permeability are allegedly constant.

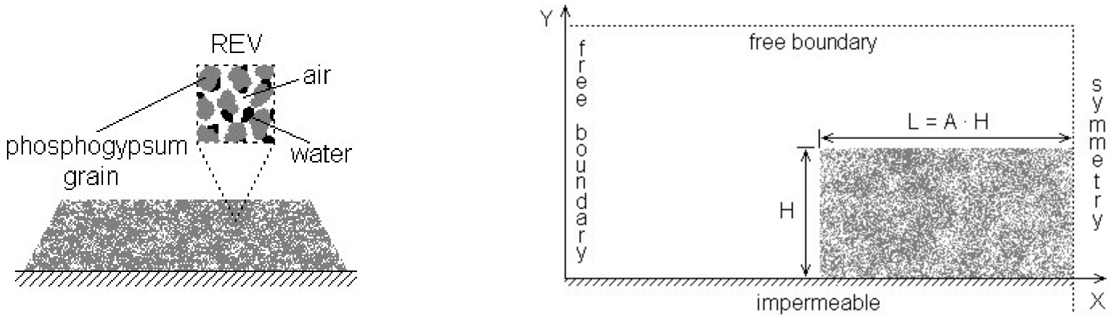

(a) (b)

Figure 1. (a) Typical composition of a REV inside a phosphogypsum stack and (b) schematic diagram and dimensionless coordinate system for the rectangular-shaped phosphogypsum stack under numerical investigation.

Local thermodynamic equilibrium is evoked so that the temperature of phosphogypsum grains and that of interstitial air are equal. Boussinesq hypothesis is assumed for the buoyancy-driven air flow, namely, all thermophysical properties are constant apart from air density for the buoyant term in vertical momentum equation, for which a linear dependence on local temperature is supposed. Adopting Darcy-Brinkman formulation (convective inertia terms included) and taking into account ^{222}Rn sources (emanation from evenly distributed ^{226}Ra particles) and sinks (^{222}Rn self decay), it has been shown elsewhere (Rabi and Mohamad, 2004a) that the steady-state two-dimensional Cartesian governing equations for bulk air mass, momentum, energy and species (^{222}Rn activity) concentration are dimensionless written as:

$$\frac{\partial U}{\partial X} + \frac{\partial V}{\partial Y} = 0 \tag{1}$$

$$U\frac{\partial U}{\partial X} + V\frac{\partial U}{\partial Y} = \Gamma^n\left(\frac{\partial^2 U}{\partial X^2} + \frac{\partial^2 U}{\partial Y^2}\right) - \frac{\partial P}{\partial X} - n\frac{U}{\mathrm{Da}} \tag{2}$$

$$U\frac{\partial V}{\partial X} + V\frac{\partial V}{\partial Y} = \Gamma^n\left(\frac{\partial^2 V}{\partial X^2} + \frac{\partial^2 V}{\partial Y^2}\right) - \frac{\partial P}{\partial Y} - n\frac{V}{\mathrm{Da}} + \mathrm{Gr}\theta \tag{3}$$

$$U\frac{\partial \theta}{\partial X} + V\frac{\partial \theta}{\partial Y} = \frac{\Lambda^n}{\mathrm{Pr}}\left(\frac{\partial^2 \theta}{\partial X^2} + \frac{\partial^2 \theta}{\partial Y^2}\right) \tag{4}$$

$$U\frac{\partial \phi}{\partial X} + V\frac{\partial \phi}{\partial Y} = \frac{\Psi^n}{\mathrm{Sc}}\left(\frac{\partial^2 \phi}{\partial X^2} + \frac{\partial^2 \phi}{\partial Y^2}\right) + \frac{1}{\mathrm{Sc}}\left[n\,\mathrm{S} - \varepsilon_c^n\,\mathrm{R}\,(\phi - \phi_0)\right] \tag{5}$$

where dimensionless variables are indicated as X and Y for Cartesian coordinates, U and V for velocity components, P for pressure, θ for temperature and ϕ for ^{222}Rn activity concentration. A dimensionless parameter n is introduced to denote whether air flows outside (n = 0) or inside (n = 1) the porous matrix (Mohamad, 2003). With respect to Eq. (5), the dimensionless activity level ϕ_0 is proportional to ^{222}Rn activity concentration in air suitably far away (Rabi and Mohamad, 2004a, 2005). The present paper assumes $\phi_0 = 0$ for the sake of simplicity. For dry phosphogypsum without grain sorption (which is presumed to be the case), the so-called partition-corrected porosity ε_c (which depends on the partitioning of radon-222 between air, water and solid grains) reduces to the ordinary stack porosity ε (Andersen, 2000).

Typical dimensionless groups related to natural-convective heat-mass transfer in porous media arise as expected, i.e., Darcy, Grashof, Prandtl and Schmidt numbers (Da, Gr, Pr, Sc). Additional dimensionless controlling parameters include bulk-to-fluid property ratios, namely for kinematic viscosity Γ, thermal diffusivity Λ and mass diffusivity Ψ (Mohamad, 2003) Apart from those parameters, Eq. (5) puts forward dimensionless groups R and S to measure the relative importance respectively of decay and of emanation in relation to diffusion, whereas a surrogate dimensionless group can be proposed as M = S/R, which is interpreted as an emanation-to-decay ratio (Rabi and Mohamad, 2004a, 2005). The aforesaid dimensionless groups are defined in terms of the stack permeability K and height H, the gravity acceleration g, air thermal expansion coefficient β, kinematic viscosity ν and thermal diffusivity α, radon-222 decay constant λ, diffusivity in open air D_o and activity generation rate $\tilde{G}$ per unit of REV, as well as scaling values ΔT and Δc for dimensionless temperature and radon-222 activity concentration, according to the following expressions:

$$\mathrm{Da} = \frac{K}{H^2} \quad , \quad \mathrm{Gr} = \frac{g\,\beta\,\Delta T\,H^3}{\nu^2} \quad , \quad \mathrm{Pr} = \frac{\nu}{\alpha} \quad , \quad \mathrm{Sc} = \frac{\nu}{D_\mathrm{o}} \quad , \quad \mathrm{R} = \frac{\lambda H^2}{D_\mathrm{o}} \quad , \quad \mathrm{S} = \frac{\tilde{G} H^2}{D_\mathrm{o}\Delta c} \tag{6}$$

For a more detailed discussion on the definitions and representative values for the previous dimensionless groups, the reader is referred to (Rabi and Mohamad, 2004a, 2005). In terms of R and M and assuming $\phi_0 = 0$, Eq. (5) is recast as:

$$U\frac{\partial\phi}{\partial X} + V\frac{\partial\phi}{\partial Y} = \frac{\Psi^n}{\mathrm{Sc}}\left(\frac{\partial^2\phi}{\partial X^2} + \frac{\partial^2\phi}{\partial Y^2}\right) + \frac{\mathrm{R}}{\mathrm{Sc}}\left(n\,\mathrm{M} - \varepsilon_\mathrm{c}^n\,\phi\right) \tag{7}$$

Solution domain comprises air and half of the phosphogypsum stack, as sketched in Fig. 1. Its top horizontal ($Y = 2$) and left vertical ($X = 0$) boundaries are free surfaces for velocity. The later is subjected to fresh (i.e., ^{222}Rn-free and "cold") incoming air while developed profiles are adopted for the former. Symmetry is assumed about the right vertical boundary ($X = 3$) and no-slip condition is applied to the impermeable ground ($Y = 0$), whose temperature underneath the stack is presumed to be higher than that of exposed ground. Furthermore, an arbitrary steep exponential drop is considered between these two temperature levels instead of a stepwise function. Wind (i.e., forced convection), pressure fluctuations or heat sources (external or internal) are disregarded in the present study. All such boundary conditions can be expressed in dimensionless form as

at $X = 0$: $$\frac{\partial U}{\partial X} = \frac{\partial V}{\partial X} = P = 0 \qquad \theta = 0 \qquad \phi = 0 \tag{8}$$

at $X = 3$: $$U = \frac{\partial V}{\partial X} = 0 \qquad \frac{\partial\theta}{\partial X} = 0 \qquad \frac{\partial\phi}{\partial X} = 0 \tag{9}$$

at $Y = 0$: $$U = V = 0 \qquad \theta = \begin{cases} \mathrm{e}^{15(X-1.5)} \ , & 0 \le X < 1.5 \\ 1 \ , & 1.5 \le X \le 3 \end{cases} \qquad \frac{\partial\phi}{\partial Y} = 0 \tag{10}$$

at $Y = 2$: $$\frac{\partial U}{\partial Y} = \frac{\partial V}{\partial Y} = P = 0 \qquad \frac{\partial\theta}{\partial Y} = 0 \qquad \frac{\partial\phi}{\partial Y} = 0 \tag{11}$$

3. Dimensionless heat-mass transfer rates and representative values for test case

As previously stated, radiation exposure assessment and radiological protection design are based on ^{222}Rn exhalation rates, taking into account both diffusive and convective fluxes (Andersen, 2000). Dimensionless (i.e., normalized) ^{222}Rn exhalation rates from top and left surfaces of the phosphogypsum stack are assessed by means of average Sherwood number. Along the lines of (Rabi and Mohamad, 2004b), the corresponding expressions are

$$\mathrm{Sh}_{\mathrm{top}} = \frac{1}{L}\int_{\mathrm{L}}\left[\frac{\mathrm{Sc}}{\Psi}V\phi - \frac{\partial\phi}{\partial Y}\right]_{\mathrm{Y=H}}\mathrm{d}X \qquad \text{and} \qquad \mathrm{Sh}_{\mathrm{left}} = -\frac{1}{H}\int_{\mathrm{H}}\left[\frac{\mathrm{Sc}}{\Psi}U\phi - \frac{\partial\phi}{\partial X}\right]_{\mathrm{X=1.5}}\mathrm{d}Y \tag{12}$$

$$\mathrm{Nu}_{\mathrm{top}} = \frac{1}{L}\int_{\mathrm{L}}\left[\frac{\mathrm{Pr}}{\Lambda}V\theta - \frac{\partial\theta}{\partial Y}\right]_{\mathrm{Y=H}}\mathrm{d}X \qquad \text{and} \qquad \mathrm{Nu}_{\mathrm{left}} = -\frac{1}{H}\int_{\mathrm{H}}\left[\frac{\mathrm{Pr}}{\Lambda}U\theta - \frac{\partial\theta}{\partial X}\right]_{\mathrm{X=1.5}}\mathrm{d}Y \tag{13}$$

whereas total counterpart numbers are simply calculated as

$$\mathrm{Sh}_{\mathrm{total}} = \mathrm{Sh}_{\mathrm{top}} + \mathrm{Sh}_{\mathrm{left}} \qquad \text{and} \qquad \mathrm{Nu}_{\mathrm{total}} = \mathrm{Nu}_{\mathrm{top}} + \mathrm{Nu}_{\mathrm{left}} \tag{14}$$

Though distinct factors concurrently influencing ^{222}Rn transport might be grouped into dimensionless parameters, a systematic analysis of the effects from each controlling parameter is unfeasible. Representative figures are thus adopted for the scenario examined: Pr = 0.71, Sc = 1.25, $\Gamma = \Lambda = 1$, $\Psi = 0.1$, R = 0.5, S = 1 and $\varepsilon_c = 0.5$ (Rabi and Mohamad, 2004b). Conversely, Grashof number is fixed at Gr = 10^7 while two Darcy numbers are assumed, namely, Da = 10^{-13} for typically compact stack and Da = 10^{-8} for extremely loose stack. In addition, this paper focuses on the effects related to the following different aspect ratios: A = 1.0, 1.5, 2.0, 2.5 and 3.0. It should be mentioned that both the solution domain dimension ($X = 3$ and $Y = 2$) and the stack left-boundary coordinate ($X = 1.5$) are kept fixed. In other words, only the stack top-boundary coordinate ($Y = H$) is allowed to vary.

4. Analytical solution for diffusion-dominated ^{222}Rn transport

Comprehensive ^{222}Rn transport in porous media does not render itself simple modeling inasmuch as it may include natural convection, transient phenomena and be extended to 3-D domains. Nazaroff *et al.* (1988) pointed to two distinct approaches to this problem: approximate analysis and numerical methods. As far as the former is concerned, analytical solutions are only feasible for limiting scenarios, although they may play a major role for numerical validation.

Recalling the low permeability of phosphogypsum stacks, a common simplification is to disregard interstitial air flow ($U \approx V \approx 0$) so that inner ^{222}Rn transfer becomes diffusion-dominated. In view of that, species equation, Eq. (5) or (7), is the single governing one whose left-hand side reduces to zero. For a vertically stratified stack, it is reasonable to suppose that considerably higher ^{222}Rn transfer rates take place along the vertical direction, i.e., $(\partial\phi/\partial Y) >> (\partial\phi/\partial X)$. The same rationale might be applied for a stack whose half-width L is significantly greater than its height H, i.e., whose aspect ratio obeys the limiting condition A >> 1. It can be readily verified that Eqs. (5) and (7) applied to points within the porous matrix (n = 1) respectively simplify to

$$\frac{d^2\phi}{dY^2} + \frac{1}{\Psi}\left(\mathrm{S} - \varepsilon_c \mathrm{R}\phi\right) = 0 \qquad \text{and} \qquad \frac{d^2\phi}{dY^2} + \frac{\mathrm{R}}{\Psi}\left(\mathrm{M} - \varepsilon_c \phi\right) = 0 \tag{15}$$

Assuming that boundary conditions for the above differential equation include impermeability at the stack base (Y = 0) as well as stack top ($Y = H$) subjected to fixed ^{222}Rn activity concentration, it can be shown (Rabi and Mohamad, 2004a) that the corresponding analytical solution is expressed as

$$\phi = \phi(Y) = \frac{\mathrm{S}}{\varepsilon_c \mathrm{R}}\left[1 - \frac{\cosh(Y\sqrt{\varepsilon_c \mathrm{R}/\Psi})}{\cosh(H\sqrt{\varepsilon_c \mathrm{R}/\Psi})}\right] = \frac{\mathrm{M}}{\varepsilon_c}\left[1 - \frac{\cosh(Y\sqrt{\varepsilon_c \mathrm{R}/\Psi})}{\cosh(H\sqrt{\varepsilon_c \mathrm{R}/\Psi})}\right] \tag{16}$$

Recalling that interstitial fluid flow was neglected ($U \approx V \approx 0$), disregarding the contribution from the left boundary and introducing the above solution into Eq. (12), the expression for average Sherwood number for a stratified stack results:

$$\mathrm{Sh}_{\mathrm{strat}} = \frac{\mathrm{S}/\Psi}{\sqrt{\varepsilon_c \mathrm{R}/\Psi}}\tanh(H\sqrt{\varepsilon_c \mathrm{R}/\Psi}) = \frac{\mathrm{M\,R}/\Psi}{\sqrt{\varepsilon_c \mathrm{R}/\Psi}}\tanh(H\sqrt{\varepsilon_c \mathrm{R}/\Psi}) \tag{17}$$

5. Numerical results and discussion

Numerical results are achieved after adapting a simulator that has been used to solve heat-mass transfer problems in media partially or fully filled with porous material (Mohamad, 2003). Governing equations are discretized following a finite-volume method on orthogonal regular grid, SIMPLER algorithm couples continuity and momentum equations and staggered grid arrangement is adopted to prevent pressure oscillations (Patankar, 1980). Algebraic equations are relaxed by TDMA algorithm and under-relaxation factors are 0.7 for U and V velocity components and set to unity for the remaining primitive dimensionless variables. Convergence is based on local and global conservation criteria within pre-established error tolerances. Details about the simulator are presented elsewhere (Mohamad, 2003).

For mesh sensitivity analysis, 5000 iterations using Da = 10^{-8} (for which convective influences are more likely to occur) and A = 1.5 were performed on the following grid refinement sequence: 77 × 52, 92 × 62, 107 × 72, 122 × 82 and 137 × 92. Table 1 presents total Nu and Sh as calculated according to Eqs. (12) through (14) and the absolute relative difference between the numerical values yielded from two consecutive mesh sizes (as distinguished by subscripts "next" and "prev"). Small differences between numerical results from successive grids are observed even for a mesh sensitivity analysis using Da = 10^{-13}, whose results are not shown for brevity but they are very similar to those in Table 1. Bearing in mind that the stack height H reduces inasmuch as the aspect ratio A increases (since the stack length L is held fixed), simulations presented in this paper were performed employing the 122 × 82 regular grid as a compromise between accuracy and computational effort.

Table 1. Total Nusselt and Sherwood numbers for mesh sensitivity analysis.

Mesh size	Number of grid points	Mesh size increase	$\mathrm{Nu}_{top} + \mathrm{Nu}_{left}$	$\left\lvert 1 - \frac{\mathrm{Nu}_{next}}{\mathrm{Nu}_{prev}} \right\rvert$	$\mathrm{Sh}_{top} + \mathrm{Sh}_{left}$	$\left\lvert 1 - \frac{\mathrm{Sh}_{next}}{\mathrm{Sh}_{prev}} \right\rvert$
77 × 52	4004		1.95		5.51	
92 × 62	5704	42.6%	1.97	1.0%	5.54	0.5%
107 × 72	7704	35.1%	1.97	0.0%	5.56	0.4%
122 × 82	10004	29.9%	2.00	1.5%	5.65	1.6%
137 × 92	12604	26.0%	2.00	0.0%	5.66	0.2%

Numerically simulated streamlines for both Da = 10^{-13} (typically packed stack) and Da = 10^{-8} (extremely loose stack) for A = 1, 2 and 3 are presented in Fig. 2. No significant differences are observed concerning the flow field as Darcy number increases from Da = 10^{-13} to Da = 10^{-8}, given the same aspect ratio. For A = 1, a recirculation cell occurs on the top of the stack whereas the flow field follows basically the same structure for the other two presented aspect ratios (A = 2 and A = 3). For all cases depicted, incoming fresh air hardly penetrates into the stack but it rather flows around the stack, being the ascending buoyancy-driven air flow essentially concentrated over the stack middle (i.e., around the symmetry line).

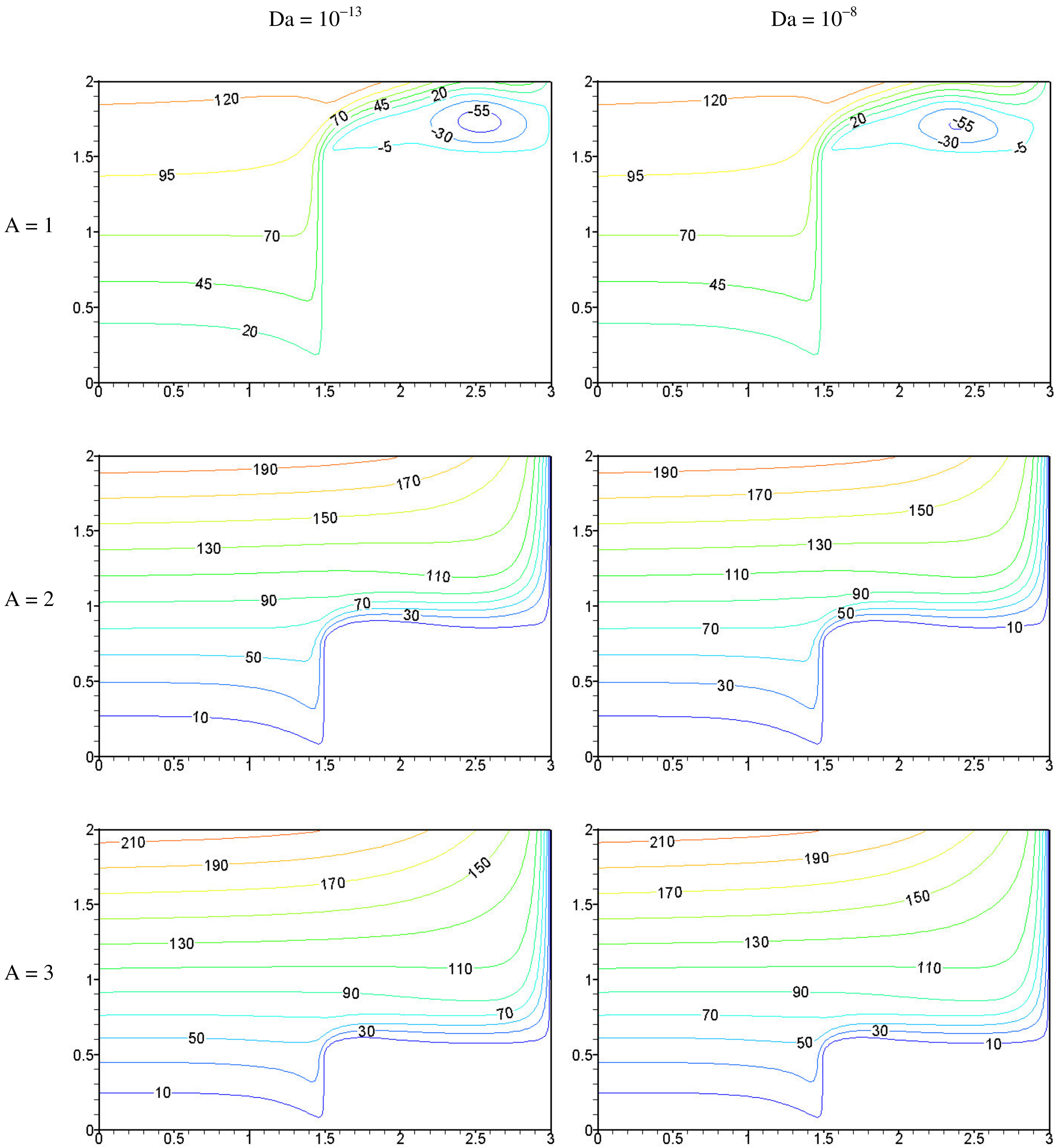

Figure 2. Numerically simulated streamlines for Da = 10^{-13} and Da = 10^{-8}, as aspect ratio increases (A = 1, 2, 3).

As a consequence, the abrupt change in permeability (by increasing Darcy number from Da = 10^{-13} up to Da = 10^{-8}) seems to barely affect either dimensionless temperature or ^{222}Rn activity concentration fields inside the stack. Figure 3 depicts both isotherms and isoconcentration lines (respectively, left and right columns) numerically simulated using only Da = 10^{-13}. The corresponding numerical results for Da = 10^{-8} are basically the same and they are here omitted for brevity. It is worth noting the unusual pattern exhibited by isoconcentration line $\phi = 1$ as well as by isotherm $\theta = 0.1$. Such isolines (and the ones in their vicinity) are rather sensitive to the streamline pattern as they are able to extend away from the stack top or to be responsive to the recirculation cell.

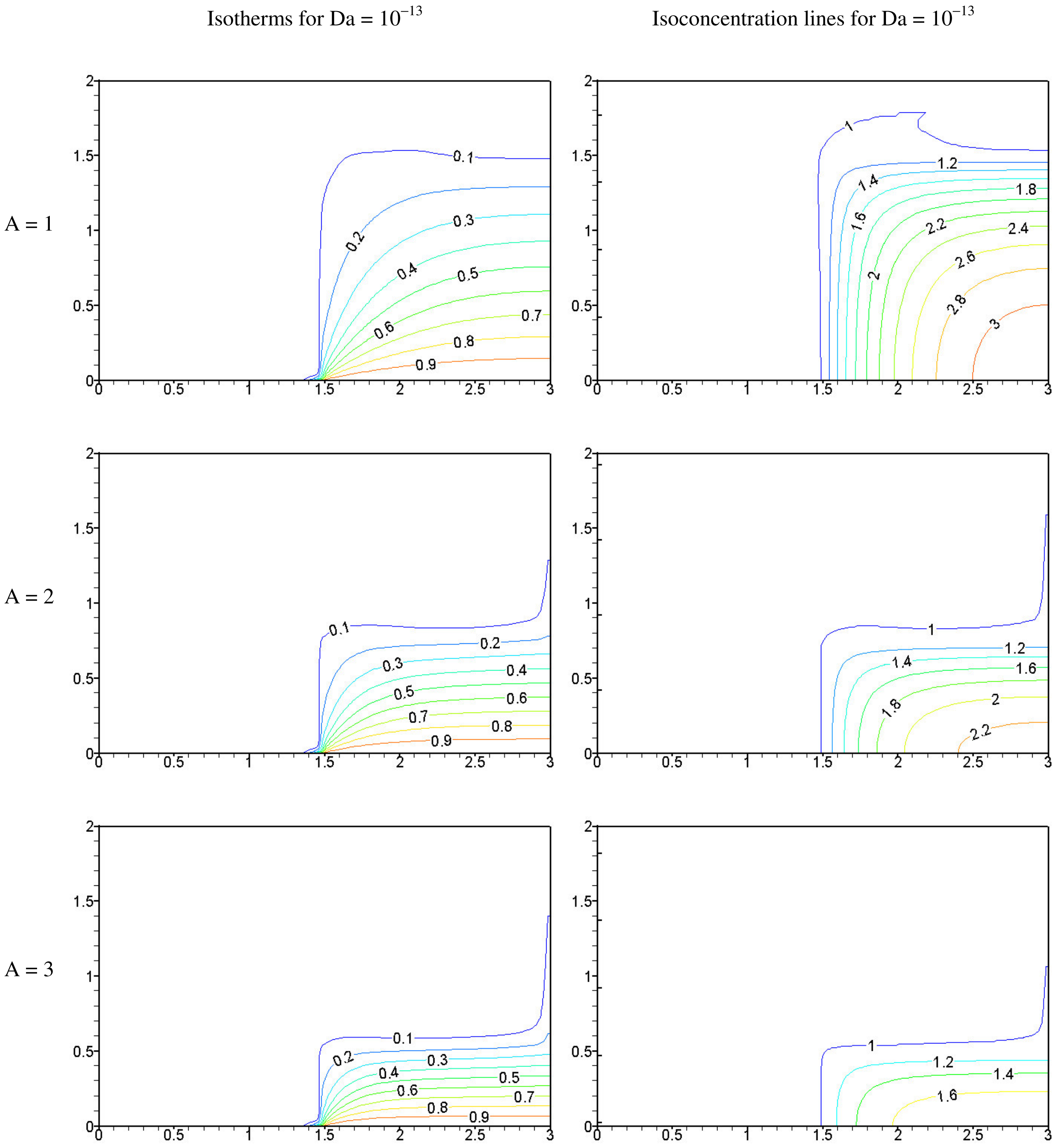

Figure 3. Numerically simulated isotherms (left column) and isoconcentration lines (right column) for Da = 10^{-13} only, as aspect ratio increases (A = 1, 2, 3). Corresponding isolines for Da = 10^{-8} are fundamentally the same.

The results for A = 1 indicate that the recirculation cell just above the stack (as observed for either Da = 10^{-13} and Da = 10^{-8}, Fig. 2) has some influence on both temperature and concentration distributions over the stack. As an attempt to check whether such recirculation is provoked by the close solution domain boundary (i.e., Y = 2), new simulations were carried out for A = 1, Da = 10^{-8} and vertically extending the solution domain up to Y = 3 and Y = 4. Figure 4 shows the corresponding simulated streamlines and it is verified that the circulation cell over the stack top still occurs. However, a deeper investigation on such issue is beyond the scope of the present paper.

A = 1 and Da = 10^{-8}

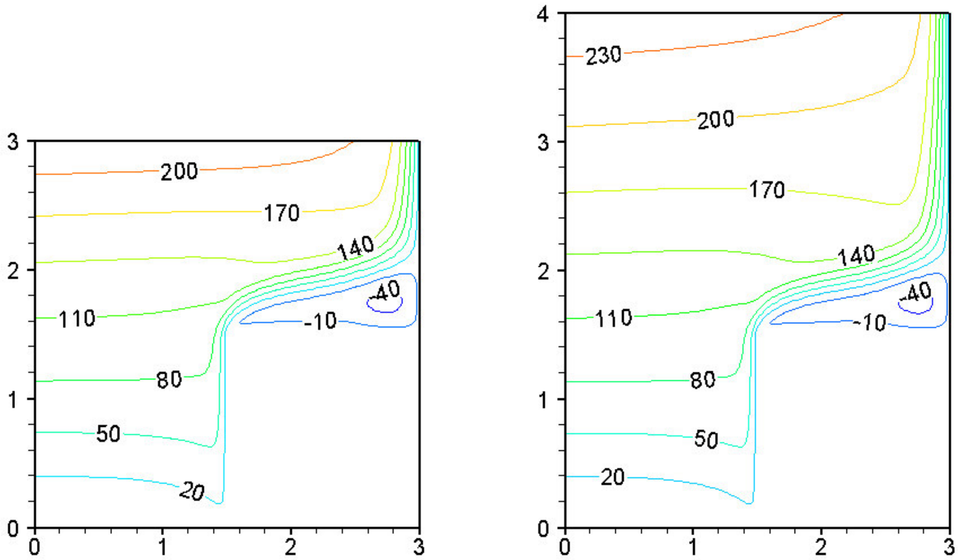

Figure 4. Numerically simulated streamlines for A= 1 and Da = 10^{-8}, as the solution domain is vertically extended.

Last but not least, Fig. 5 compares analytical (i.e., stratified-stack) average Sherwood numbers, Sh_{strat} as given by Eq. (17), to their numerical counterparts, Sh_{top} and Sh_{total} as calculated by Eqs. (12) and (14), concerning contribution from stack top boundary and total value (= top + left), for all aspect ratios, A = 1.0, 1.5, 2.0, 2.5 and 3.0, and Darcy numbers, Da = 10^{-13} and Da = 10^{-8}, investigated in the present paper. It is worth remembering that the stack half-width was held fixed at L = 1.5 in all cases simulated so that the stack height $H = L/A$ is the variable one, which is properly introduced in Eq. (17) along with $\Psi = 0.1$, R = 0.5, S = 1 and $\varepsilon_c = 0.5$.

It is observed that Sh_{strat}, Sh_{total} and Sh_{top} notably reduce inasmuch as H diminishes (or, equivalently, as A increases). Because L is fixed, this is basically due to the reduction of the stack volume and consequently due to the reduction of the amount of exhaling porous material (i.e., phosphogypsum). Besides being sensitive to the quantity of material, Sh_{total} is additionally proportional to the stack height H as it comprises contribution from Sh_{left}. Since Sh_{total} is two-fold sensitive to H, a faster decrease is verified particularly related to more permeable stacks (Da = 10^{-8}). For such relatively loose stacks, incoming fresh air from left penetrates slightly more (as compared to the infiltration into less permeable counterparts, Da = 10^{-13}), which corresponds to a larger negative "contribution" from Sh_{left}, as indicated by Eq. (12).

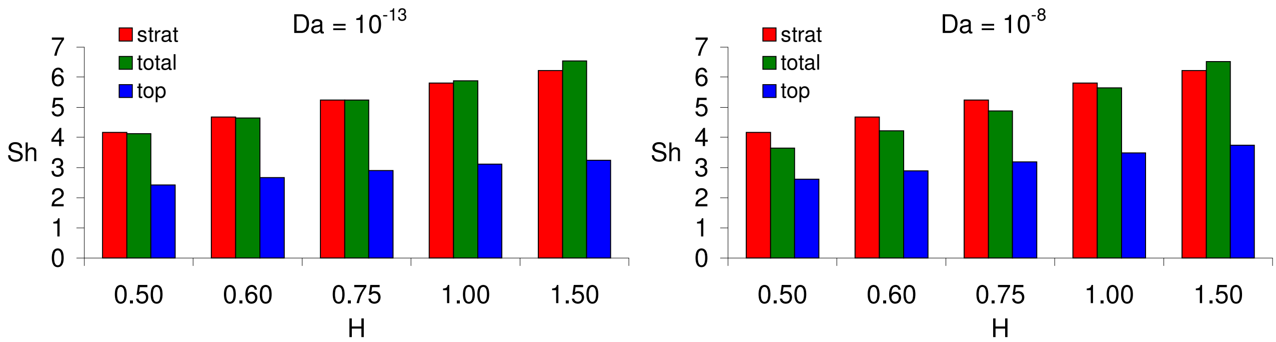

(a) (b)

Figure 5. Average Sherwood numbers for stratified-stack (analytical expression) and numerically simulated at stack top boundary and total value (top + left boundaries) for Da = 10^{-13} and Da = 10^{-8} and different stack heights.

Moreover, Fig. 5 also depicts the expected trend that Sh_{strat}, Sh_{total} and Sh_{top} will converge to the same value as $H \to 0$ (i.e., for A >> 1), since Sh_{left} becomes more and more suppressed. Recalling that $\tanh(x) \to x$ as $x \to 0$, Eq. (17) provides such limiting value, namely,

$$Sh_{H\to 0} = \frac{S\,H}{\Psi} = \frac{M\,R\,H}{\Psi} \tag{18}$$

6. Concluding remarks

Radon-222 exhalation from phosphogypsum entails many physical parameters and comprehensive approach is likely to rely on numerical methods. This paper outlines dimensionless model equations for ^{222}Rn transport from a rectangular dry phosphogypsum stack, which are numerically solved by means of an adapted finite-volume simulator that has been successfully used to solve heat and mass transfer problems in solution domains partially or fully filled up with porous material. Allegedly laminar buoyancy-driven air flow is modeled following Darcy-Brinkman-Boussinesq approach. Effects due to different aspect ratios are investigated for two Darcy numbers, which are related to a typically packed stack and to a hypothetical relatively loose stack. The remaining controlling dimensionless parameters are fixed at representative values.

Stratified ^{222}Rn transport is a limiting scenario for which negligible interstitial air flow is a required assumption. A corresponding analytical solution was deduced for boundary conditions including null activity concentration at the stack top and no-flux condition (impermeability) at its base. For this particular case, an analytical expression for the average Sherwood number could be properly inferred (which measures normalized ^{222}Rn exhalation rates).

For each aspect ratio investigated, similar streamlines were numerically simulated for both Darcy numbers, so that isotherms and isoconcentration lines remained roughly unchanged inside the phosphogypsum stack. Although this indicates that ^{222}Rn transport is diffusion-dominated, stratification can only be observed for stacks whose (half-)width is considerably larger than its height (i.e., whose aspect ratio tends to infinity). Nevertheless, ^{222}Rn transport through the stack side boundary might compensate differences from Sherwood numbers as calculated at the stack top boundary (alone) and from the stratified (analytical) concentration distribution.

7. Acknowledgement

The author is grateful to Dr. Giovana Tommaso (FZEA / USP) for her remarks when writing the present paper.

8. References

Andersen, C.E., 2000, "Radon Transport Modelling: User's Guide to RnMod3d", Riso -R-1201(EN), Riso National Laboratory, Roskilde, Denmark.

Loureiro, C.O., 1987, "Simulation of the steady-state transport of radon from soil into houses with basements under constant negative pressure", PhD. thesis, Environmental Health Sciences, University of Michigan, Ann Arbor, USA.

Mohamad, A.A., 2003, "Heat transfer enhancements in heat exchangers fitted with porous media Part I: constant wall temperature", International Journal of Thermal Sciences, vol. 42, pp. 385-395.

Nazaroff, W.W., Moed, B.A., Sextro, R.G., 1988, "Soil as a source of indoor radon: generation, migration and entry". IN: Nazaroff, W.W., Nero, A.V. (eds.), "Radon and its Decay Products in Indoor Air", John Wiley & Sons, New York, USA.

Nero, A.V., 1988, "Radon and its decay products in indoor air: an overview". IN: Nazaroff, W.W., Nero, A.V. (eds.), "Radon and its Decay Products in Indoor Air", John Wiley & Sons, New York, USA.

Patankar, S.V., 1980, "Numerical Heat Transfer and Fluid Flow", Hemisphere, New York, USA .

Rabi, J.A., Mohamad, A.A., 2004a, "Prediction of ^{222}Rn exhalation rates from phosphogypsum-based stacks. Part I: parametric mathematical modeling", Proceedings of the 10th Brazilian Congress of Thermal Sciences and Engineering – ENCIT 2004, Rio de Janeiro, Brazil, paper CIT04-0442, CD-ROM.

Rabi, J.A., Mohamad, A.A., 2004b, "Prediction of ^{222}Rn exhalation rates from phosphogypsum-based stacks. Part II: preliminary numerical results", Proceedings of the 10th Brazilian Congress of Thermal Sciences and Engineering – ENCIT 2004, Rio de Janeiro, Brazil, paper CIT04-0443, CD-ROM.

Rabi, J.A., Mohamad, A.A., 2005, "Radon-222 exhalation rates from phosphogypsum-bearing embankment subjected to constant temperature and fixed activity concentration", Journal of Porous Media, vol. 8, n. 2, pp. 175-191.

Riley, W.J., Robinson, A.L., Gadgil, A.J., Nazaroff, W.W., 1999, "Effects of variable wind speed and direction on radon transport from soil into buildings: model development and exploratory results", Atmospheric Environment, vol. 33, pp. 2157-2168.

UNSCEAR – United Nations Scientific Committee on the Effects of Atomic Radiation, 2000, "Sources and Effects of Ionizing Radiation", New York, U.N.

Yu, C., Loureiro, C.O., Cheng, J.J., Jones, L.G., Wang, Y.Y., Chia, Y.P., Faillace, E., 1993, "Data Collection Handbook to Support Modeling Impacts of Radioactive Materials in Soil", Environmental Assessment and Information Sciences Division, Argonne National Laboratory, Argonne, USA.

9. Responsibility notice

The author is the only responsible for the printed material included in this paper.